

Matt Pharr is a junior at Rice University where he is pursuing a double major in mechanical engineering and materials science. He participated in the Science Undergraduate Laboratory Internships (SULI) program in the summer of 2005 at ORNL where he tested properties of silicon carbide for potential use in nuclear fusion and fission reactors. This coming summer he will be doing an internship at the University of Tennessee where he will be examining scintillation materials for use in SPECT/CT/PET scanners. He plans to attend graduate school to earn a PhD in either mechanical engineering or materials science.

Yutai Katoh is a Staff Scientist at Oak Ridge National Laboratory's Materials Science and Technology Division. He received his PhD in materials science from the University of Tokyo and he was Associate Professor of Advanced Energy Materials at Kyoto University for seven years. He specializes

in advanced ceramics and composites for energy system applications and is in charge of several DOE fusion and advanced nuclear materials programs. His current research includes development and characterization of ceramic composites for severe environment applications; neutron and high energy particle irradiation effects in metals, alloys and ceramics; and helium effect on irradiation-induced phenomena in metals and ceramics.

Hongbin Bei is currently a Postdoctoral Research Associate at Department of Materials Science and Engineering at the University of Tennessee. He received his PhD in materials science and engineering from the University of Tennessee at Knoxville in 2003, working on directional solidification of intermetallics for high temperature application. His current research includes synthesis of intermetallic composites with well-controlled microstructures and investigation of their small-scale mechanical behavior.

DEPENDENCE OF FRACTURE TOUGHNESS ON CRYSTALLOGRAPHIC ORIENTATION IN SINGLE-CRYSTALLINE CUBIC (β) SILICON CARBIDE

MATT PHARR, YUTAI KATOH, AND HONGBEN BEI

ABSTRACT

Along with other desirable properties, the ability of silicon carbide (SiC) to retain high strength after elevated temperature exposures to neutron irradiation renders it potentially applicable in fusion and advanced fission reactors. However, properties of the material such as room temperature fracture toughness must be thoroughly characterized prior to such practical applications. The objective of this work is to investigate the dependence of fracture toughness on crystallographic orientation for single-crystalline β -SiC. X-ray diffraction was first performed on the samples to determine the orientation of the crystal. Nanoindentation was used to determine a hardness of 39.1 and 35.2 GPa and elastic modulus of 474 and 446 GPa for the single-crystalline and polycrystalline samples, respectively. Additionally, crack lengths and indentation diagonals were measured via a Vickers micro-hardness indenter under a load of 100 gf for different crystallographic orientations with indentation diagonals aligned along fundamental cleavage planes. Upon examination of propagation direction of cracks, the cracks usually did not initiate and propagate from the corners of the indentation where the stresses are concentrated but instead from the indentation sides. Such cracks clearly moved along the $\{1\ 1\ 0\}$ family of planes (previously determined to be preferred cleavage plane), demonstrating that the fracture toughness of SiC is comparatively so much lower along this set of planes that the lower energy required to cleave along this plane overpowers the stress-concentration at indentation corners. Additionally, fracture toughness in the $\langle 1\ 1\ 0 \rangle$ direction was $1.84\ \text{MPa}\cdot\text{m}^{1/2}$, lower than the $3.46\ \text{MPa}\cdot\text{m}^{1/2}$ measured for polycrystalline SiC (which can serve as an average of a spectrum of orientations), further demonstrating that single-crystalline β -SiC has a strong fracture toughness anisotropy.

INTRODUCTION

For the last three decades, silicon carbide (SiC) has been considered a promising candidate for use in nuclear fusion and fission reactors [1-5]. Desirable properties of SiC for such applications include high strength and chemical stabilities [1], low density, low neutron activation [2], and safety at high temperatures [3]. However, before this material is implemented into such nuclear reactors, much care must be taken in extensively examining its properties.

One such property in need of examination is that of room temperature fracture toughness, as SiC demonstrates a relatively low one, with a maximum for polycrystalline SiC of $\sim 4\ \text{MPa}\cdot\text{m}^{1/2}$ [6-7]. Although basic fracture properties have previously been

measured, fracture toughness as a function of spatial orientation has not yet been investigated. Such investigation is important in fully characterizing the fracture properties of SiC, as stresses applied along a certain cleavage plane (in a single-crystalline material) may yield a different value for fracture toughness than would be observed along a different cleavage plane. This phenomenon is related to the number of bonds broken per unit area along different cleavage planes. Since more energy is required to break more bonds, higher fracture toughness is expected along cleavage planes with a higher bond density. Thus, in this study we investigate the crystallographic orientation dependence of fracture toughness in single-crystalline β -(cubic or 3C) SiC.

MATERIALS AND METHODS

Specimen description, preparation, and initial examination

Two different forms of SiC were examined. The first was a 200-micron-thick sample of single-crystalline β -SiC (Hoya Advanced Semiconductor Technologies Co, Ltd.). These crystals were grown as described by H. Nagasawa et al. [8], using an “Undulant-Si” substrate and a process that eliminates most planar defects. Laue back-scattered x-ray diffraction revealed the orientation of the flat edge of the sample, allowing for alignment relative to certain cleavage planes. The other sample was a 2.54-mm-thick film of polycrystalline chemical-vapor-deposited (CVD) SiC. This sample was included to provide direct comparison to the properties associated with fracture toughness in the single-crystalline sample.

Both of these were grinded down to their desired thicknesses. To finalize the preparation of the samples, they were polished using a diamond powder slurry. This polishing process increases the optical reflectivity of the surface so that the crack length can be more accurately measured [10]. Additionally, polishing may eliminate problems associated with initial surface stresses, as a compressive initial surface stress would decrease crack length while a tensile surface stress would do just the opposite [10]. The samples were then mounted to a cylindrical piece of aluminum using CrystalBond™.

Vickers indentation

A micro-indenter with a Vickers tip was used as it has many pertinent advantages as described by Ponton and Rawlings [9]. Primarily, it can be used on a very small sample, proving highly important as the single-crystalline sample was only 200 microns thick. Further advantages include quickness of experimentation and cost effectiveness [9]. However, the most important advantage is that associated with the shape of the indenter. For the single-crystalline sample, it was crucial to implement an indenter that could potentially activate key cleavage planes. In a cubic structure, the shape of the Vickers indenter (a diamond shape with corners situated 90° apart) is highly conducive to cleavage along certain fundamental planes. Additionally, to more easily attempt this activation along key cleavage planes, a rotating stage was implemented. This stage contained 360 degree marks on the circumference so that the sample could be easily rotated by a specified angle.

The samples were first tested with a 2001 Micromet™ (Buehler, Ltd.) Vickers micro-hardness tester. Indentations were performed on each sample at a load of 100 gf for a dwell time of 15 s. Since the single-crystalline sample was relatively thin, a small load was used to help prevent crack breakthrough. However, a load lower than 100 gf was not employed, as crack measurement at such loads is highly difficult and a slight error in determination of crack length has a more significant impact on fracture toughness estimation at these lower loads.

The single-crystalline specimen was first observed under an optical microscope so that the indentation corners were aligned with the $\{1\ 0\ 0\}$ plane. Then, a series of indentations was made at this orientation. Crack lengths and indentation diameters were measured

with an optical microscope immediately after indentation to prevent the effect of time dependent slow-crack propagation. A model of the lengths measured is included in Figure 1. As suggested by Osborne, et al., these indentations were spaced both away from the edges of

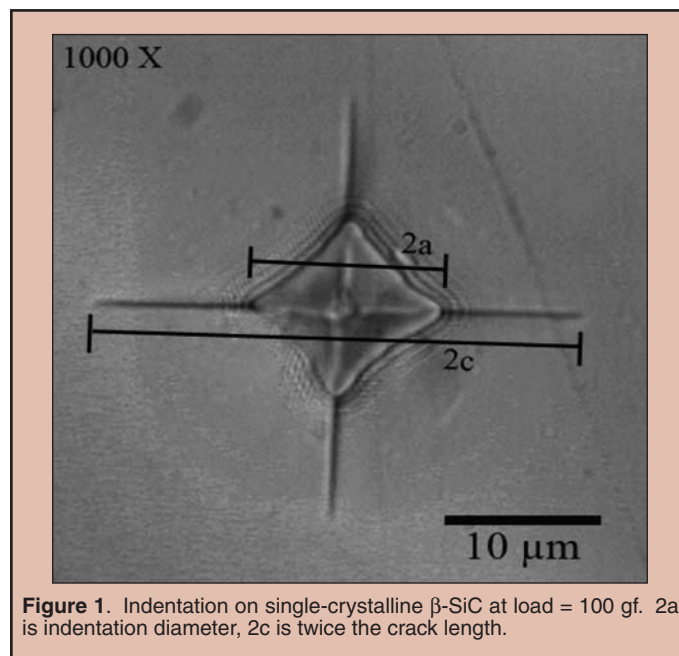


Figure 1. Indentation on single-crystalline β -SiC at load = 100 gf. 2a is indentation diameter, 2c is twice the crack length.

the sample and from one another to prevent possible influence from another indentation or edge [2]. The specimen was then rotated (clockwise) by 22.5° and another series of indentations was made to activate the $\{2\ 1\ 0\}$ family of cleavage planes. Finally, the specimen was rotated (clockwise) by an additional 22.5° and a final series of indentations was made to activate the $\{1\ 1\ 0\}$ cleavage plane. At least five indentations were made at each orientation depending on whether or not crack lengths could clearly be observed. There was no need to rotate the polycrystalline SiC sample. Thus, the procedure simply consisted of making about ten indentations and measuring crack and indentation diameter lengths.

Nanoindentation

Nanoindentation was performed on both samples to determine hardness and elastic modulus by means of a Nanoindenter XP (Nano-instruments, Oak Ridge, TN) equipped with a Berkovich tip. 50-micron-thick single-crystalline and polycrystalline samples were used as larger samples were not necessary since chance of crack breakthrough and effect of substrate can be avoided with such small indentation depths. These samples were mounted with Crystalbond™ on a piece of sapphire was to increase the stiffness. The Oliver and Pharr [14] method was used to calculate the hardness and modulus of the samples. The Berkovich indenter and machine stiffness were carefully calibrated by testing a standard sample of fused quartz. The continuous stiffness mode (CSM) was used in all tests with a maximum depth of 500 nm. Elastic modulus and hardness for each sample were then obtained by taking averages of numerous indentations over the range of a 100-200 nm indentation

depth. This depth was deep enough to avoid problems associated with surface roughness of the specimen and shallow enough that the substrate did not begin to significantly impact the properties of the specimen.

RESULTS AND DISCUSSION

Method used for measurement of fracture toughness

Fracture toughness can be estimated through one of many models present today. Ponton and Rawlings state that the best “all-around” models are those that display the ability to correlate K_{IC} and K_{IC} and demonstrate the best correlating ability as regards five main material classes [10]. After extensive examination into which models appear to work the best, Ponton and Rawlings [10] conclude that the best “all-around” equations are those of the Evans and Charles [11] equation, the Evans and Davis equation [12], and the Shetty, Wright, Mincer, and Clauer equation [13]. However, specifically for SiC, Osborne et al. [2] state that the Evans and Davis equation is quite appropriate. Even though there is no real evidence that models based on half-penny cracks model half-penny cracks as opposed to Palmqvist cracks (as is modeled by Shetty, Wright, Mincer, and Clauer). Thus, for the purposes of this experiment, the Evans and Davis equation will be used and is as follows:

where the indentation half-diameter and crack length are represented by ‘a’ and ‘c’, respectively, as shown in Figure 1; K_{IC} is the fracture

$$K_{IC} = H_V \sqrt{a} \left(\frac{E}{H_V} \right)^{2/5} \times 10^F \quad (1a)$$

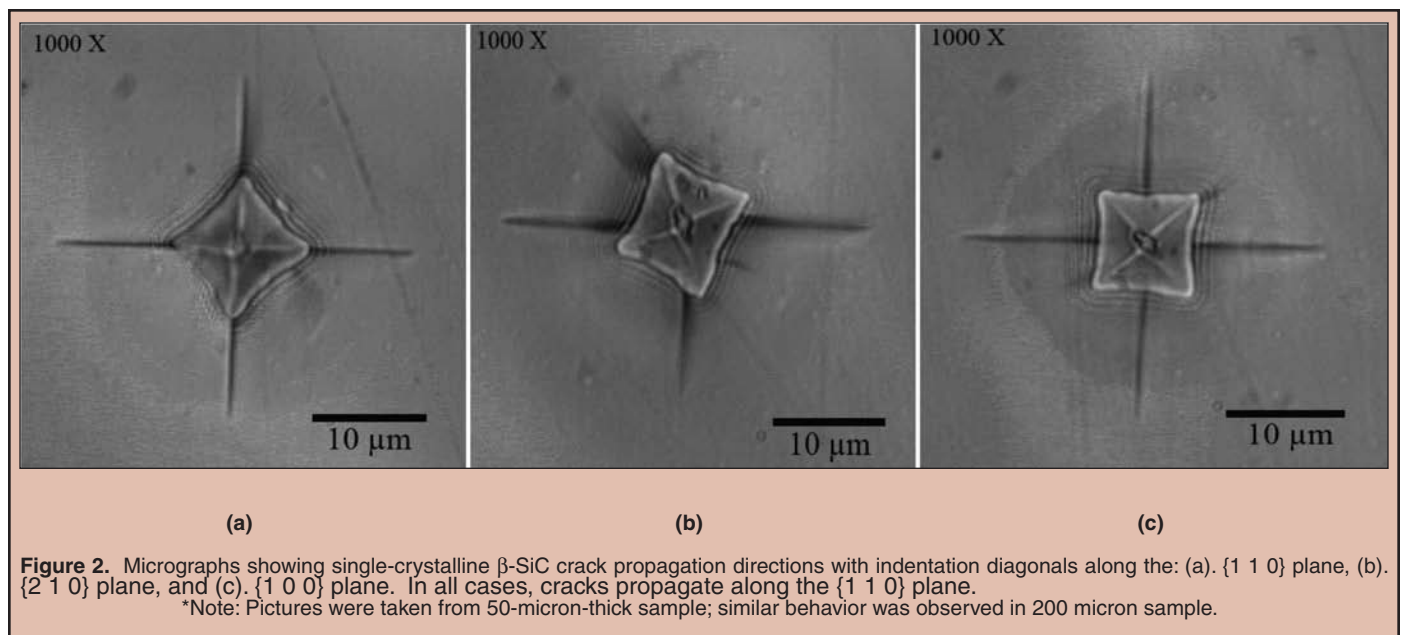
$$F = -1.59 - .34B - 2.02B^2 + 11.23B^3 - 24.97B^4 + 16.32B^5 \quad (1b)$$

$$B = \log_{10} \left(\frac{c}{a} \right) \quad (1c)$$

toughness (or critical stress intensity factor); H_V is the Vickers Hardness; and E is the elastic modulus. The relationship between the nano-hardness and the Vickers hardness is found by simple geometric conversion, which is $H_V = .9272 H_{nano}$ [9].

Fracture anisotropy in single-crystalline β -SiC

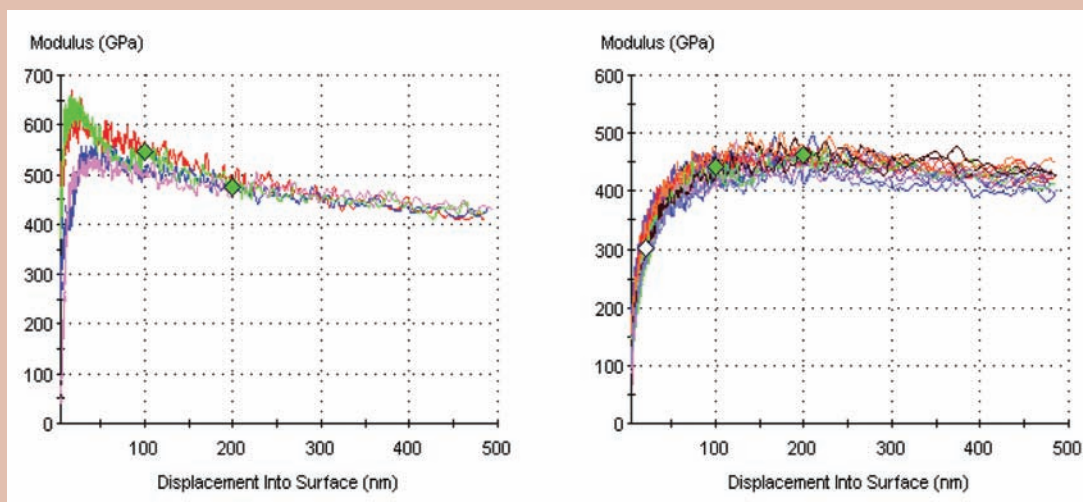
Predictions for fracture toughness were based on the notion that different cleavage planes have different bond densities. Since more energy is required to break more bonds, cleavage planes with higher bond densities should demonstrate higher fracture toughness. Based on the crystal structure of β -SiC (zincblende cubic structure), it was predicted that within the planes normal to the {1 0 0} surface, fracture toughness would be lowest along the {1 1 0} plane, highest along the {1 0 0} plane, and somewhere in-between for the {2 1 0} plane. However, only activation of the {1 1 0} plane was obtained with Vickers indentation testing, as shown in Figure 2. This figure demonstrates that although indentation corners were aligned with different cleavage planes, actual crack propagation did not occur along those desired planes. Thus, the fracture of the single-crystalline sample exhibits very strong crystallographic orientation dependence, as cracks tend to propagate along the preferred cleavage plane, the {1 1 0}, even with higher stress concentration along other planes. Unfortunately, quantifying this dependence proves impossible with the method used as the Evans and Davis equation is based on a wedge-shaped indentation with cracks propagating from indentation corners (as they do not except along the preferred cleavage plane). However, it is important to note that Table 1 demonstrates similar crack length at each orientation despite the cracks not propagating as the Evans and Davis method suggests. Thus, the assumed mechanism may not be exactly responsible for the observed crack extension.



Crystal Type	Degree of Rotation from {1 1 0} plane	Average Crack Length (μm)	Std. Dev.	Average Indentation Diameter (μm)	Std. Dev.	Average Fracture Toughness ($\text{MPa}\cdot\text{m}^{1/2}$)	Std. Dev.
Single	0	11.60	.569	6.42	.231	1.84	.200
Single	22.5	11.59	.398	6.61	.116	1.95*	.122
Single	45	11.88	.510	6.85	.009	2.02*	.131
Poly	N/A	8.81	.608	8.5	.266	3.46	.156

* - indicates that the following cracks do not propagate along the assumed plane and thus do not follow the method used.

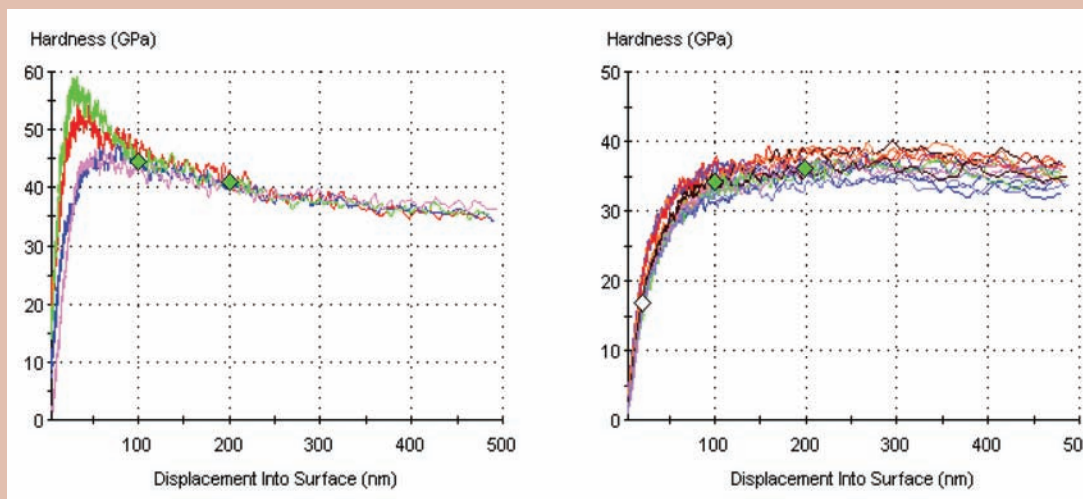
Table 1: Results of micro-indentation with load = 100 gf. Fracture Toughness values were obtained by Eq. (1).



(a) Single-Crystalline Sample

(b) Polycrystalline sample

Figure 3. Determination of elastic modulus in the (a) single-crystalline and (b) polycrystalline samples. Averages were taken over the 100 nm to 200 nm depth range.



(a) Single-Crystalline Sample

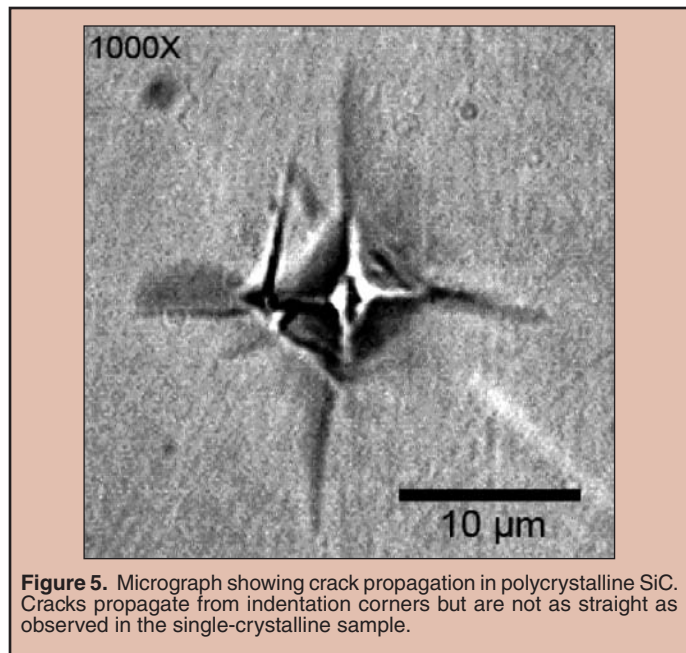
(b) Polycrystalline Sample

Figure 4. Determination of nano-hardness in the (a) single-crystalline and (b) polycrystalline samples. Averages were taken over the 100 nm to 200 nm indentation depth range.

Comparison between single-crystalline and polycrystalline samples

Despite the model not being appropriate for each of the orientations within the single-crystalline sample, since cracks did propagate from indentation corners in the $\langle 1\ 1\ 0 \rangle$ direction, it can be used for comparison between the single-crystalline and polycrystalline samples. For the single-crystalline sample, nanoindentation gave an elastic modulus of ~ 474 GPa and a hardness of ~ 39.1 GPa (Figures 3a,4a).

For the polycrystalline sample, nano-indentation gave an elastic modulus of ~ 446 GPa and a hardness of ~ 35.2 GPa (Figures 3b,4b), indicating a crystallographic orientation dependence of elastic modulus. The results of plugging these and the corresponding crack/indentation diameter lengths into equation (1) are given in Table 1. The important numbers are that of fracture toughness, ~ 1.84 $\text{MPa}\cdot\text{m}^{1/2}$ for the single-crystalline sample as opposed to ~ 3.46 $\text{MPa}\cdot\text{m}^{1/2}$ for the polycrystalline sample (Table 1). Furthermore, comparison of the cracks in the $\langle 1\ 1\ 0 \rangle$ direction in the single-crystalline sample and the cracks in the polycrystalline samples (Figures 2, 5) demonstrates that the cracks are straighter in the single-crystalline sample. This deflection found in the polycrystalline sample may show that the cracks are deflecting as to move along cleavage planes with lower bond densities, further demonstrating



the orientation dependence of fracture toughness. Unfortunately, it is hard to tell if this deflection is occurring at each grain boundary as it is difficult to determine exactly where the cracks are actually deflecting. However, even if these cracks are not deflecting at each grain boundary, the polycrystalline sample should serve somewhat as an average of all crystallographic orientations possible on a $\{1\ 0\ 0\}$ surface. Thus, the lower fracture toughness found along the preferred cleavage plane in the single-crystalline is sample consistent with the supposition that fracture toughness should be lower along planes with lower bond densities.

CONCLUSIONS

Fracture morphology demonstrated that cracks did not initiate from indentation corners. Thus, the cleavage planes were not activated as desired, making direct comparison of fracture toughness data obtained at each angle of rotation invalid according to the assumed model. However, this morphology did demonstrate that strong dependence on crystallographic orientation does exist as the cracks clearly initiated and propagated along a preferred cleavage plane despite higher stress concentration along other planes. Additionally, the fracture toughness of the single-crystalline sample along the preferred cleavage plane was much lower than the polycrystalline sample, further demonstrating that fracture toughness does strongly depend on the crystallographic orientation.

ACKNOWLEDGMENTS

This project was performed at Oak Ridge National Laboratory in Oak Ridge, Tennessee. I would like to thank the United States Department of Energy Office of Science for providing funding for the Summer Undergraduate Laboratory Internship (SULI) program that allowed my participation in this rewarding internship. I would additionally like to thank my mentor, Yutai Katoh for his scientific expertise, guidance, and willingness to answer my numerous questions. Special thanks is extended to Hongbin Bei for his help with the micro-indentation and x-ray diffraction equipment and this paper and to Andrei Rar for his help with the nano-indentation equipment.

REFERENCES

- [1] A. R. Raffray, R. Jones, G. Aiello, M. Billone, L. Giancarli, H. Golfier, A. Hasegawa, Y. Katoh, A. Kohyama, S. Nishio, B. Riccardi, and M.S. Tillack "Design and material issues for high performance SiC_f/SiC-based fusion power cores," *Fusion and Engineering Design*, 55 [1] 55-95 (2001).
- [2] M. Osborne, J. Hay, L. L. Snead, and D. Steiner, "Mechanical- and physical-property changes of neutron-irradiated chemical-vapor-deposited silicon carbide," *Journal of the American Ceramic Society*, 82 [9] 2490-2496 (1999).
- [3] R. H. Jones, L. Giancarli, A. Hasegawa, Y. Katoh, A. Kohyama, B. Riccardi, L. L. Snead, and W. J. Weber "Promises and Challenges of SiC_f/SiC composites for fusion energy applications," *Journal of Nuclear Materials*, 307, 1057-1072 (2002).
- [4] T. Noda, A. Kohyama, and Y. Katoh, "Recent progress of SiC-fibers and SiC/SiC-composites for fusion applications," *Physica Scripta*, 91, 24-29 (2001).
- [5] R. H. Jones, D. Steiner, H. L. Heinisch, G. A. Newsome, and H. M. Kerch, "Radiation Resistant Ceramic Matrix Composites," *Journal of Nuclear Materials*, 245, 87-107 (1997).
- [6] H. Kodama and T. Miyoshi, "Study of Fracture Behavior of Very Fine-Grained Silicon Carbide Ceramics," *Journal of the American Ceramic Society*, 73 [10] 3081 (1990).
- [7] K. Niihara, "Mechanical Properties of Chemically Vapor Deposited Nonoxide Ceramics," *American Ceramic Society Bulletin*, 63 [9] 1160-1164 (1984).
- [8] H. Nagasawa, K. Yagi, and T. Kawahara "3C-SiC hetero-epitaxial growth on undulant Si(0 0 1) substrate," *Journal of Crystal Growth*, 237, 1244-1249.
- [9] C. B. Ponton and R. D. Rawlings, "Vickers indentation fracture toughness test-part 1-Review of literature and formulation of standardized indentation toughness equations," *Materials Science and Technology*, 5, 865-872 (1989).
- [10] C. B. Ponton and R. D. Rawlings, "Vickers indentation fracture toughness test-part 2-application and critical evaluation of standardised indentation toughness equations," *Materials Science and Technology*, 5, 961-976 (1989).
- [11] A. G. Evans and E. A. Charles, "Fracture Toughness Determinations by Indentations," *Journal of the American Ceramic Society*, 59 [7-8] 371-372 (1976).
- [12] A. G. Evans, "Fracture Toughness: The Role of Indentation Techniques," pp. 112-135 in *Fracture Mechanics Applied to Brittle Materials*. Edited by S. W. Freiman, American Society for Testing and Materials, Philadelphia, PA, 1979.
- [13] D. K. Shetty, I. G. Wright, P. N. Mincer, and A. H. Clauer, "Indentation Fracture of WC-Co Cermets," *Journal of Materials Science*, 20, [5] 1873-1882 (1985).
- [14] W.C. Oliver and G. M. Pharr, "An Improved Technique for Determining Hardness and Elastic Modulus Using Load and Displacement Sensing Indentation Experiments," *Journal of Materials Research*, 20, 1564-1583 (1992).